Quantum Electronics **35** (1) 85 – 90 (2005)

LASER APPLICATIONS AND OTHER TOPICS IN QUANTUM ELECTRONICS

PACS numbers: 42.30.Va; 43.35.Sx; 42.79.Jq
DOI: 10.1070/QE2005v035n01ABEH002782

Acousto-optic image processing in coherent light

V.I. Balakshy, V.B. Voloshinov

***Abstract*. The results of recent studies on coherent acousto-optic image processing performed at the chair of physics of oscillations at the Department of Physics of Moscow State University are reported. It is shown that this processing method is based on the filtration of the spatial spectrum of an optical signal in an acousto-optic cell. The main attention is paid to the analysis of the dependence of the transfer function of the cell on the crystal cut, geometry of acousto-optic interaction, and acoustic-wave parameters. It is shown that an acousto-optic cell allows the image differentiation and integration as well as the visualisation of phase objects. The results of experiments and computer simulation are presented which illustrate the possibilities of acousto-optic image processing.**

Keywords: *acousto-optic interaction, Bragg diffraction, coherent transfer function, spatial filtration, optical data processing, visualisation of phase objects, image edge enhancement.*

1. Introduction

At present acousto-optic (AO) methods for controlling optical radiation find wide applications in various fields of science and technology. The AO interaction is used to control the amplitude, frequency, phase, and polarisation of a light wave and to change its propagation direction [1 – 4]. The AO modulators, deflectors, and filters are characterised by a fast response, low control voltages, high reliability, and simple design. These advantages provided their wide applications not only in laser physics but also in ecology, medicine, and military devices.

The application of the AO interaction is not restricted to the above-mentioned devices. One of the directions of modern acousto-optics is optical image processing with the help of the acoustic wave acting on the amplitude and phase structures of the image. These studies were pioneered by researchers at the chair of physics of oscillations at the Department of Physics of Moscow State University in the 1980s [5 – 10]. It was shown in these papers that under certain conditions an AO cell acts on a light wave propagating through it as a linear filter of spatial frequencies. The transfer function of such a filter characterises the selective properties of the AO interaction. The form of the transfer function and, hence, the law of image transformation depend on the acoustic-beam structure and the AO interaction geometry. It was shown that an AO cell can be used for classical image processing such as differentiation and integration, as well as for the visualisation of phase objects [9 – 11]. Compared to other image processing methods [12], the AO method offers a number of advantages. The AO spatial filters are insensitive to their location in an optical system, they do not require a careful adjustment and an additional optics to perform the spatial Fourier transform. However, the main advantage of such filters is their simplicity and rapid tuning (by varying the acoustic-wave parameters), which allows the real-time data processing.

The subsequent experimental studies performed in our country [13 – 15] and abroad [16 – 20] confirmed the high efficiency of the AO image-processing method. In these experiments, both the zero- and first-order Bragg diffraction was used. Two-dimensional images were processed by using either two crossed AO cells placed in series or one cell with a special geometry of the AO interaction.

In this paper, we report the results of our recent studies on AO image processing. The main attention is paid to the choice of the optimal geometry of the AO interaction. Both the experimental results and examples of computer simulations are presented.

2. Transfer function of an AO cell

Figure 1 illustrates one of the possible schemes of AO image processing. Lens (*1*) transfers the light field formed by object (*2*) to detection plane (*3*). The image-carrying light wave propagates through AO cell (*4*) and diffracts in the acoustic field produced by piezoelectric transducer (*5*). In the Bragg diffraction regime, which is assumed in our analysis, the spectrum of diffracted radiation has only two maxima of the zero and first orders. The place of the AO cell in the system is not critical, it is important only that no vignetting of the light beam by a finite aperture of the cell occurred.

Because the AO interaction is linear with respect to the light field, we can use the spectral method [3, 12] to describe the propagation of an arbitrary light beam through the AO cell. When a monochromatic acoustic wave with the frequency Ω and wave number $K = \Omega/V = 2\pi f/V$ (where

V.I. Balakshy, V.B. Voloshinov Department of Physics, M.V. Lomonosov Moscow State University, Vorob'evy gory, 119992 Moscow, Russia; e-mail: balakshy@phys.msu.ru, volosh@phys.msu.ru

Received 12 July 2004; revision received 24 November 2004
Kvantovaya Elektronika **35** (1) 85 – 90 (2005)
Translated by M.N. Sapozhnikov

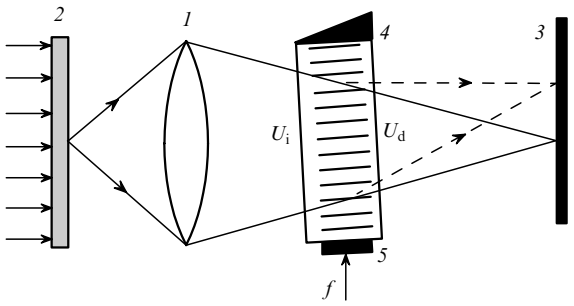

Figure 1. Principal scheme for AO image processing: (*1*) lens; (*2*) transparency; (*3*) recording plane; (*4*) AO cell; (*5*) piezoelectric transducer.

V is the sound speed) propagates in the call along the z axis, the spatial spectra of the incident (U_i) and diffracted (U_d) radiation are related by the expression [2, 6]

$$U_d(\vartheta_d) = \exp(j\Omega t)\int_{-\infty}^{\infty} U_i(\vartheta_i)H_a^{(1)}(\vartheta_i) \times \delta\left(\vartheta_d - \frac{K}{k} - \vartheta_i\right)d\vartheta_i, \quad (1)$$

where ϑ_i and ϑ_d are the angles in the AO interaction plane xz measured from the x axis; $k = 2\pi n/\lambda$ is the wave number of light; λ is the wavelength of the light wave in vacuum; n is the refractive index; and j is the imaginary unit.

Expression (1) allows one to treat the AO cell as a linear optical system with the transfer function $H_a^{(1)}$. This is not a usual system, similar to those employed for optical data processing [12]. Apart from the spatial filtration of an optical signal, the AO cell shifts the signal spectrum as a whole along the axis of temporal frequencies by Ω (due to the Doppler effect) and along the axis of spatial frequencies $f_z = n\vartheta_i/\lambda$ by $K/2\pi$. The shift along the temporal-frequency axis is described by the factor $\exp(j\Omega t)$, while the shift along the spatial-frequency axis is described by the integral in (1).

In the Bragg diffraction regime, when the diffraction spectrum consists of only two maxima (of the zero and first orders), the transfer function is determined by the expression

$$H_a^{(1)}(\vartheta_i) = -\frac{A}{2}\mathrm{sinc}\left[\frac{(A^2 + R^2)^{1/2}}{2\pi}\right], \quad (2)$$

where A is the Raman–Nath parameter proportional to the acoustic-wave amplitude; $R = \eta l = Kl(\vartheta_i - \vartheta_B)$ is the dimensionless mismatch; l is the width of the acoustic beam in the AO interaction plane xz; ϑ_B is the Bragg angle; and $\mathrm{sinc}(x) \equiv \sin\pi x/\pi x$. Physically, the transfer function is the angular characteristic of the AO interaction. Therefore, the filtering properties of the cell are determined by the angular selectivity of the AO effect. When the diffraction efficiency is low, expression (2) is simplified:

$$H_a^{(1)}(\vartheta_i) = -\frac{A}{2}\mathrm{sinc}\frac{R}{2\pi} = -\frac{A}{2}\mathrm{sinc}\left[\frac{Kl}{2\pi}(\vartheta_i - \vartheta_B)\right]. \quad (3)$$

The transfer function allows one to determine the transmission band $\Delta f_z = n\Delta\vartheta_i/\lambda$ of spatial frequencies and the minimal size of a resolved image element formed in the diffracted beam:

$$\Delta\vartheta_i = 0.89\frac{V}{lf} = 0.89\varphi_s, \quad d_{\min} = 1.22\frac{\lambda lf}{nV} = 1.22\frac{\lambda}{n\varphi_s}, \quad (4)$$

where $\varphi_s = V/lf$ is the angle of divergence of the acoustic beam in the xz plane. For example, for typical parameters $l = 0.5$ cm, $f = 100$ MHz, $n = 2$, $V = 3 \times 10^5$ cm s^{-1}, and $\lambda = 0.6$ μm, we have $d_{\min} = 0.056$ mm (spatial resolution is 18 lines mm^{-1}). This means that for any optics and any linear aperture of the AO cell, it is impossible to obtain in the diffracted beam an image of the better quality because spectral components carrying information on the smaller details of the initial image will propagate through the cell without diffraction. An increase in the ultrasound frequency f enhances the AO selectivity, resulting in the narrowing of the angular range $\Delta\vartheta_i$ of the cell and deteriorating of the spatial resolution.

The appearance of the divergence φ_s of the acoustic beam in expressions (4) is not accidental because it is known [2] that the angular characteristic of the AO interaction in the case of low diffraction efficiency is the radiation pattern of a sound source. Therefore, by varying the structure of a piezoelectric transducer, one can obtain different transfer functions of the AO cell. In a strong acoustic field, the transfer function is distorted. As follows from expression (2), the angular range $\Delta\vartheta_i$ narrows down with increasing acoustic power, however, in the interval $0 < A < \pi$, which is of most interest for practice, this effect does not exceed 10 %.

In the strong AO interaction regime, the zero-order diffraction can be also used for spatial image filtering. The zero-order transfer function has the form [6]

$$H_a^{(0)}(\vartheta_i) = \left\{\cos\left[\frac{(A^2 + R^2)^{1/2}}{2}\right] - j\frac{R}{2}\mathrm{sinc}\left[\frac{(A^2 + R^2)^{1/2}}{2\pi}\right]\right\}\exp\left(j\frac{R}{2}\right). \quad (5)$$

Note that, unlike the first-order function, the function $H_a^{(0)}$ is complex. This means that not only the amplitude but also the phase structure of the image changes during the propagation of a light beam through the AO cell. The modulus and argument of the function $H_a^{(0)}$ are shown in Fig. 2.

3. Tangential geometry of the AO interaction

All the results presented above are valid when the refractive indices of the incident (n_i) and diffracted (n_d) light are independent of the angles of incidence (ϑ_i) and diffraction (ϑ_d). The main specific feature of this variant is that the angular range $\Delta\vartheta_i$ is independent of the AO interaction geometry but is determined only by the divergence φ_s of ultrasound. In most cases of isotropic and anisotropic diffraction [2], this approximation is quite acceptable because the range $\Delta\vartheta_i$ does not exceed, as a rule, several degrees. The exception is the region of the so-called tangential geometry, where $d\vartheta_B/df \to \infty$.

Let us denote by f_t the frequency at which $df/d\vartheta_B = 0$, and the corresponding Bragg angle by $\vartheta_B^{(t)}$. Then, by introducing the dimensionless parameters

$$Q = 2\pi\frac{\lambda lf_t^2}{nV^2}, \quad F = \frac{f}{f_t},$$

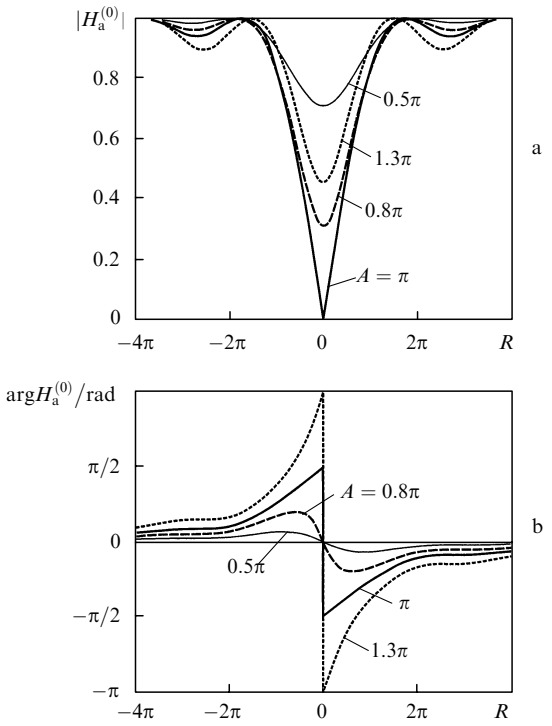

Figure 2. Modulus (a) and argument (b) of the transfer functions for the zero-order Bragg diffraction for different values of the Raman–Nath parameter A.

$$\Theta = \vartheta \Big/ \frac{\lambda f_t}{2nV}, \quad N_i'' = \frac{1}{n_i}\frac{d^2 n_i}{d\vartheta_i^2}\Big|_{\vartheta_B^{(t)}}, \tag{6}$$

we obtain the expression

$$H_a^{(1)}(\Theta_i) = -\frac{A}{2}\operatorname{sinc}\frac{R}{2\pi} = -\frac{A}{2}\operatorname{sinc}\left\{\frac{Q}{4\pi}[(F^2-1) + (F-1)\Theta_i + \frac{N_i''}{4}(\Theta_i - \Theta_B^{(t)})^2]\right\} \tag{7}$$

for the first-order transfer function [2]. The phase-matching condition $R = 0$ gives the frequency dependence of the Bragg angle:

$$\Theta_B(F) = \left[\Theta_B^{(t)}\frac{2(F-1)}{N_i''}\right] \times \left\{1 \pm \left[1 - N_i''\frac{N_i''\Theta_B^{(t)2} + 4(F^2-1)}{[N_i''\Theta_B^{(t)} - 2(F-1)]^2}\right]^{1/2}\right\}. \tag{8}$$

This dependence for the tangential region is shown in Fig. 3a by the solid curve. For $F > 1$, the curve has two branches, which correspond to the signs '$\pm$' in expression (8). The two dashed curves restrict the transmission region of the AO cell at the 3-dB level. (The boundaries of the transmission region are constructed for $Q = 2\pi$.) The calculation was performed for the case of anisotropic diffraction in a paratellurite crystal (TeO_2), when the AO interaction plane makes the angle $\alpha = 14^\circ$ with the optic axis. For this cut of the crystal, $f_t = 67.7$ MHz, $\vartheta_B^{(t)} = -15.3^\circ$, $\Theta_B^{(t)} = -17.5$, and $N_i'' = 0.103$ (for $\lambda = 0.63$ μm).

Figure 3b shows the first-order transfer functions calculated from (7) for different ultrasonic frequencies. These

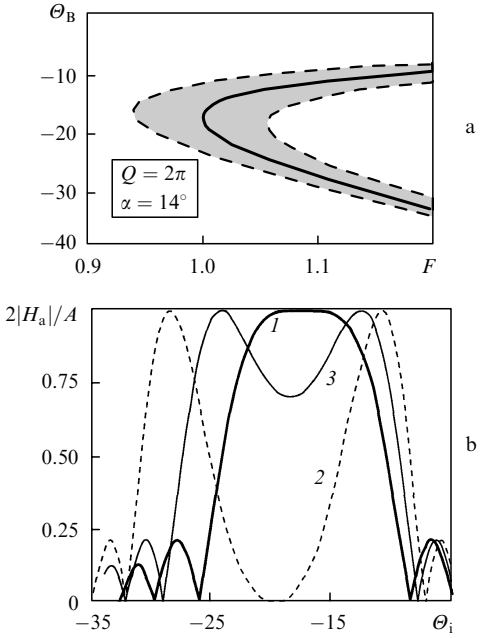

Figure 3. Tangential geometry of the AO interaction in a paratellurite crystal: (a) transmission region of the AO cell; (b) transfer functions for $F = 1$ (*1*), 1.122 (*2*), and 1.057 (*3*).

functions differ substantially from the function described by expression (1). The AO cell introduces minimal distortions to the optical signal for $F = 1$, when the transfer function has a flat top [curve (*1*)]. In this case, the angular range of the cell is $\Delta\Theta_i^{(t)} = 9.5/(Q|N_i''|)^{1/2}$. As F increases, a hole appears at the centre of the transfer function, and for $F > F_m$, where $F_m = 1 - 5.6/[Q(\Theta_B^{(t)} + 2)]$, the angular range divides into two regions [curve (*2*)], whose widths rapidly decrease with increasing frequency, approaching the values determined by expression (4). The broadest range is achieved when $F = F_m$ [curve (*3*)]. This range is broader than the region in the case of usual interaction geometry by a factor of 58.

A weak angular selectivity is a specific feature of the tangential geometry, which has found application in non-collinear AO videofilters used to select images over wavelengths [21]. From the point of view of spatial filtration of images, this geometry is also very attractive because it allows one to filter either low [curve (*1*)] or high [curve (*2*)] spatial frequencies [7, 8]. In the first case, the integrated output image is obtained, while in the second case – the differentiated output image. Note that the passage from one law of image processing to the other in the system can be performed very rapidly, for a few microseconds, i.e., for the time required for the establishment of an acoustic wave at a new frequency in the cell.

4. Spatial filtration of two-dimensional images

The processing of two-dimensional images by AO methods has a number of specific features caused by the fact that the selectivity of the AO effect is manifested, as a rule, only in the interaction plane. Figure 4a shows the two-dimensional transfer functions $H_a^{(1)}(\vartheta_i, \chi)$ in the case of the AO interaction in an isotropic medium. The angle ϑ_i is measured, as above, in the xz interaction plane, while the angle χ is measured in the xy orthogonal plane. The

picture brightness at each point is proportional to $|H_a^{(1)}|$. The centre of the picture corresponds to the zero spatial frequency. The bright bow-shaped band corresponds to the region of spatial frequencies $f_z = n\vartheta_i/\lambda$ and $f_y = n\chi/\lambda$ transmitted by the cell. The section of this region by a vertical straight line gives the function $|H_a^{(1)}(\vartheta_i)|$ described by expression (3). Two weak bow-shaped bands are the side lobes of the function sinc. It is clear from Fig. 4a that in this case the cell performs the one-dimensional filtration of the optical signal in the xz plane because the spatial-frequency selectivity in the xy plane is virtually absent. Therefore, to perform two-dimensional filtration, it is necessary either to use two crossed cells placed in series or to excite two acoustic waves in orthogonal directions in the cell [17–19].

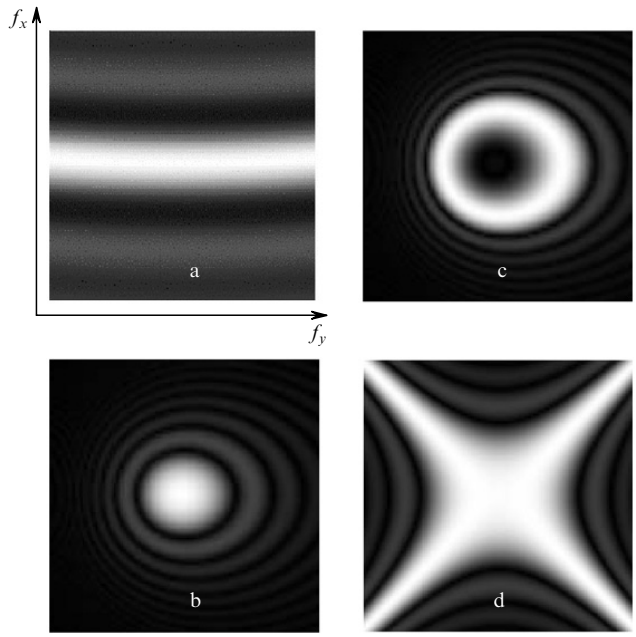

Figure 4. Two-dimensional transfer functions: (a) isotropic medium; (b, c) anisotropic diffraction, tangential geometry; (d) anisotropic diffraction, collinear geometry.

We proposed in papers [7, 8, 14, 15, 22] to process two-dimensional images by using special AO interaction geometries, which can be realised only upon anisotropic diffraction. In this case, only one cell is used for image processing. One of the possible variants is the tangential geometry considered above. In this case, the angular selectivity is virtually the same in the interaction plane and in the orthogonal plane. For this reason, the transfer function is almost axially symmetric (see Figs 4b, c). The transfer function can be calculated from expression (2) with the mismatch R described by the expression [15]

$$R = \frac{2\pi l}{\lambda}\left[- n_i \sin\vartheta_i \pm \left(n_d^2 - n_i^2\cos^2\vartheta_i\right)^{1/2} - \frac{\lambda f}{V}\right], \qquad (9)$$

where the dependences of the refractive indices n_i and n_d on the angles ϑ_i, ϑ_d and χ should be taken into account in the general case. The calculation was performed for a calcium molybdate $CaMoO_4$ crystal. The transfer functions in Figs 4b and c differ in the ultrasonic frequency (49.3 and 49.6 MHz) and correspond to one-dimensional characteristics (*1*) and (*2*) in Fig. 3b. Therefore, the passage from the image integration to image differentiation regime in the AO spatial filtration system does not require a change of a spatial filter, as in the classical scheme [12]; it is sufficient to change the ultrasonic frequency only by 0.3 MHz.

Another variant of the AO interaction of interest for image processing takes place upon quasi-collinear diffraction [2], when the interacting beams propagate perpendicular to the optic axis of a uniaxial crystal. In this case, the mismatch is described by the expression

$$R = \frac{2\pi l}{\lambda}\left\{ n_i\cos\vartheta_i \mp \left[n_d^2 - \left(n_i \sin\vartheta_i + \frac{\lambda f}{V}\right)^2\right]^{1/2}\right\}, \qquad (10)$$

where l is the cell length in the direction of ultrasound propagation. At the collinear phase matching frequency $f_c = |n_d - n_i|V/\lambda$, the transfer function has the form of a cross with rays oriented at the angles $\pm 45^\circ$ to the optic axis (Fig. 4d). In this case, a selective differentiation of the image along the y or z axis is possible.

5. Computer simulations

In this section, we present the results of computer simulations of the image processing by the method of AO spatial filtering. As an object, we considered an opaque screen with three identical equidistantly located rectangular holes (Fig. 5a). The spectrum of the input optical signal found with the help of the fast Fourier transform (FFT) was multiplied by the transfer function and then the output image was calculated by using the inverse FFT.

Figure 5b illustrates the case of the transfer function shown in Fig. 4b. In this variant, the AO cell transmits the high-frequency components of the optical spectrum, resul-

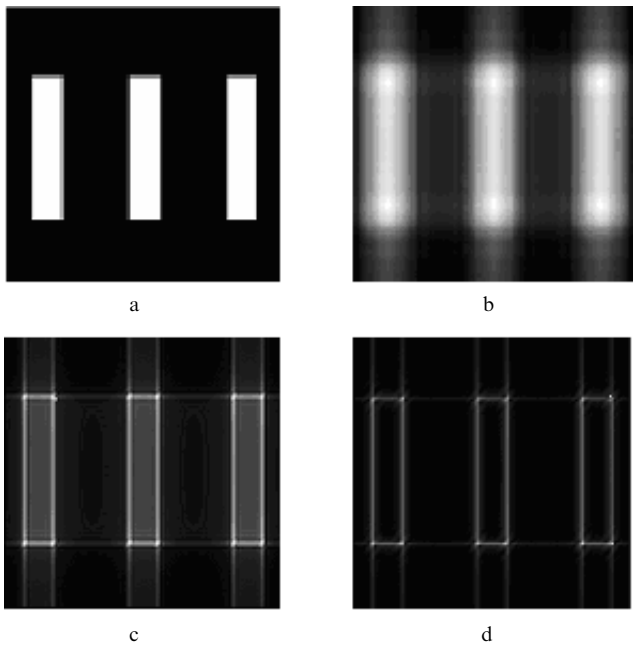

Figure 5. Computer simulations of AO image processing: (a) initial image; (b) output image in the first diffraction order for the transfer function shown in Fig. 4b; (c) output image in the first diffraction order for the transfer function shown in Fig. 4c; (d) output image in the zero diffraction order for the variant in Fig. 4b.

ting in the smoothing of sharp intensity variations. Such an image transformation corresponds to the integration procedure. As the ultrasonic frequency increases, the transformation law changes. In the case 4c, the zero component of the spectrum is completely suppressed, and only high-frequency components undergo diffraction. As a result, the regions of sharp intensity variations are emphasised in the output image and the so-called image edge enhancement effect appears (Fig. 5c). This effect is even more distinct in the zero-order diffraction (Fig. 5d).

6. Experimental results

The results presented below were obtained by using an AO cell made of a paratellurite crystal. The cell operated in the region of tangential geometry. The shear acoustic wave was excited in the $(1\bar{1}0)$ plane at an angle of 81.4° to the optic axis. For this cut of the crystal, $f_t = 97.9$ MHz and the Bragg angle is $\vartheta_B^{(t)} = 11.3°$ (for $\lambda = 0.63$ μm). A piezoelectric transducer had $l = 1.0$ cm in the interaction plane and $b = 0.6$ cm in the orthogonal plane. Therefore, the linear aperture of the cell was 0.6×1.0 cm, while the time constant of the cell, determining the speed of the cell response, was 16 μs. The light beam from a He–Ne laser expanded by a telescope illuminated a slide with an image recorded in it. This image was then projected by the input lens on the cell plane. The output lens formed the processed image on the screen or on the input window of a CCD array.

Figure 6 shows the initial and filtered optical signals illustrating the operation of the system in the image differentiation regime. In this case, the light beam was incident on the cell at the Bragg angle, and the ultrasonic power at the frequency f_t was selected so that the diffraction efficiency for the axial component of the beam was close to 100 %. This provided virtually complete suppression of the zero-order spectral component in the zero-order diffraction. For other components, the transmission of the filter increased with their removing from the beam axis, resulting in the image edge enhancement.

a b

Figure 6. Experimental results: (a) initial image; (b) output image in the zero diffraction order.

7. Visualisation of phase objects

A light wave propagating through an object or reflecting from it is modulated in the general case both by the amplitude and phase. However, an eye or any other photosensitive device is capable of detecting only a change in the intensity (amplitude) of light. Therefore, all the information about the object contained in the phase modulation is lost in usual observation methods, although it can be very important and sometimes (for phase objects) the only information about the object. To record the phase modulation of light, it should be first transformed to the amplitude one.

The problem of recording the phase structure of light fields (or in other words, the visualisation of phase objects) belongs to the classical problems of wave optics. Recent interest in this problem is caused by the development of laser physics and adaptive optics. There exist several methods for visualising phase objects: shadow, phase-contrast, interference, etc. [12]. Some of them are based on the spatial filtration of an optical signal in the Fourier plane. Thus, in the dark-field method, the zero component of the signal spectrum is eliminated with the help of a screen, in the phase-contrast method, this component is phase-shifted by $\pi/2$, while in the curl method, half the Fourier plane is screened.

We proposed [9–11] and studied a new method for the visualisation of phase objects, based on the filtering properties of the AO cell. Depending on the transfer function, this method allows the use of different laws of the transformation of the light-wave phase to its intensity. The passage from one law to another does not require the readjustment of the system and can be performed for a few microseconds. The possibilities of the method are illustrated below by computer simulations.

We assumed in the simulations that a phase object is a perfectly transparent glass plate homogeneous over its thickness on which three identical rectangular glass plates are laid over (the phase analogue of an amplitude object shown in Fig. 5a). Figure 7a shows at the left the transfer function of the zero-order diffraction for the tangential geometry, while the visualised image is at the right. In fact,

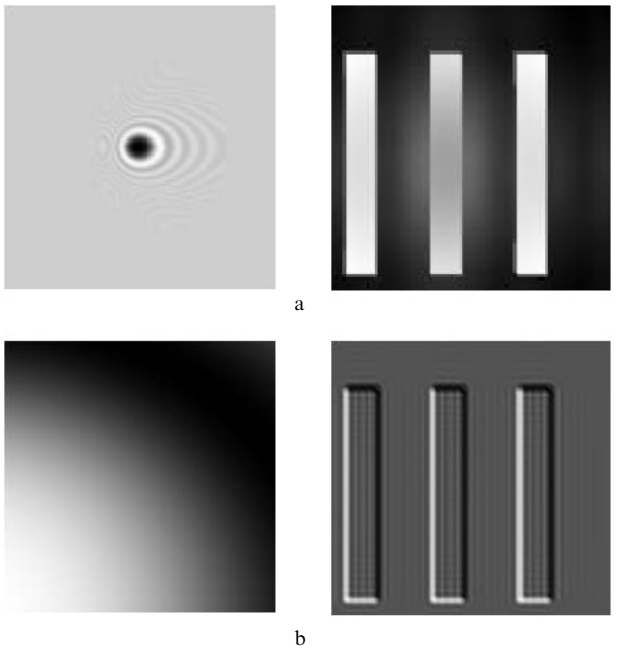

a b

Figure 7. Computer simulations of the AO visualisation of phase objects (the transfer function is at the left, the visualised image at the right); (a) dark-field visualisation; (b) phase-gradient visualisation.

we are dealing here with the AO analogue of the dark-field method because the zero component is completely removed from the optical signal spectrum. The intensity at each point of the visualised image is proportional to the square of the light-field phase. However, if the working point is shifted to the slope of the transfer function (Fig. 7b, at the left), the visualised image drastically changes (Fig. 7b, at the right). In this case, the distribution of the light intensity at the output is proportional to the phase gradient in the direction of the gradient of the transfer function. One can clearly see that the positive and negative values of the gradient are visualised differently, and the picture as a whole represents a pseudo-volume image of the wave front of the initial light wave.

8. Conclusions

We have reported briefly the study of the AO image processing method based on the selective properties of Bragg diffraction. This method allows one to perform easily the differentiation and integration of images and to visualise the wave front of a light wave. The passage from one regime to another can be rapidly performed by varying the parameters of an acoustic wave excited in the AO cell. The type of processing is determined by the transfer function of the cell, which depends both on the structure of a piezoelectric transducer and the crystal cut, the AO interaction geometry, and the frequency and amplitude of the acoustic wave.

In fact, the AO method is a method for coherent image processing because it allows the control both of the amplitude and phase structure of the light field. Its principal difference from the rest of the methods for coherent processing is that the AO cell directly acts on the angular spectrum of the optical signal, so that there is no need to form this spectrum with the help of a Fourier lens, while the cell itself can be placed at different places in the beam, provided that the beam is not vignetted by a finite aperture of the cell.

Acknowledgements. This work was partially supported by the Russian Foundation for Basic Research (Grant No. 02-07-90448).

References

1. Magdich L.N., Molchanov V.Ya. *Acoustooptic Devices and Their Applications* (New York: Gordon Breach, 1988; Moscow: Sov. Radio, 1978).
2. Balakshy V.I., Parygin V.N., Chirkov L.E. *Fizicheskie osnovy akustooptiki (*Physical Foundations of Acousto-optics) (Moscow: Radio i Svyaz', 1985).
3. Parygin V.N., Balakshy V.I. *Opticheskaya obrabotka informatsii* (Optical Data Processing) (Moscow: Izd. Mosk. Univ., 1987).
4. Korpel A. *Akustooptika* (Acoustooptics) (Moscow: Mir, 1993).
5. Balakshy V.I. *Trudy seminara 'Metody i sredstva obrabotki opticheskoi informatsii'* (Proc. of Seminar on Methods and Devices for Optical Data Processing) (Moscow: Znanie, 1983) p. 139.
6. Balakshy V.I. *Radiotekh. Radioelektron.*, **29**, 1610 (1984).
7. Voloshinov V.B., Balakshy V.I., Belikov I.B., et al. USSR Inventor's Certificate No. 1378620 (1987).
8. Voloshinov V.B., Belikov I.B., Balakshy V.I., Parygin V.N. USSR Inventor's Certificate No. 1436686 (1988).
9. Balakshy V.I., Kukushkin A.G. *Opt. Spektrosk.*, **64**, 99 (1988).
10. Balakshy V.I., Grigorov S.D., Kolosov M.A. *Opt. Spektrosk.*, **68**, 1381 (1990).
11. Balakshy V.I. *Opt. Laser Techn.*, **28**, 109 (1996).
12. Goodman J.W. *Introduction to Fourier Optics* (New York: McGraw-Hill, 1968; Moscow: Mir, 1970).
13. Voloshinov V.B., Babkina T.M. *Pure Appl. Opt.*, **3**, S54 (2001).
14. Voloshinov V.B., Molchanov V.Ya., Babkina T.M. *Opt. Eng.*, **41**, 1273 (2002).
15. Balakshy V.I., Voloshinov V.B., Babkina T.M., Kostyuk D.E. *J. Modern Opt.*, **52**, 1 (2005).
16. Banerjee P.P., Cao D., Gibbs P.M., Poon T.-C. *Proc. SPIE Int. Soc. Opt. Eng.*, **2463**, 158 (1995).
17. Xia J., Dunn D., Poon T.-C., Banerjee P.P. *Opt. Commun.*, **128**, 1 (1996).
18. Banerjee P.P., Cao D., Poon T.-C. *Appl. Opt.*, **36**, 3086 (1997).
19. Banerjee P.P., Poon T.-C. *Proc. SPIE Int. Soc. Opt. Eng.*, **3581**, 48 (1998).
20. Cao D., Banerjee P.P., Poon T.-C. *Appl. Opt.*, **37**, 3007 (1998).
21. Voloshinov V.B. *Proc. SPIE Int. Soc. Opt. Eng.*, **3584**, 116 (1998).
22. Balakshy V.I., Asratyan K.R., Molchanov V.Ya. *Pure Appl. Opt.*, **3**, S87 (2001).